

CELLULOSE NANOCRYSTALS ISOLATED FROM BEAN SEED HULLS: ACETYLATION AND CHARACTERIZATION.

ABSTRACT

Bean seed hulls is an agro-waste with abundant content of lignocellulosic materials but are being wasted due to its underutilization. Cellulose nanocrystals (CNCs) were successfully extracted from bean seed hulls using alkali treatment, bleaching and sulphuric acid hydrolysis. Cellulose triacetate (CTA) was obtained from CNCs by acetylation using acetic anhydride with sulphuric acid as catalyst. CNCs is neutral pH whereas CTA is slightly acidic. CNCs was sparingly soluble in ethanol but CTA was completely soluble in ethanol. CTA has a higher melting point than CNCs. The density of both CNCs and CTA is approximately equal to the density of water. SEM analysis revealed that CNCs is irregular and fragmented in nature and has both more large surface area and porosity than CTA. FTIR analysis showed the presence of the dominant functional groups such as O-H stretch, N-H stretch, C-H stretch, C-O stretch and C-N stretch in both CNCs and CTA. GC-MS analysis revealed the presence of the prevalent organic compounds such as alkanes, alcohols, phenols, alkanones, phthalates, carboxylic acids, esters and triterpene in both CNCs and CTA. Therefore, the isolation of CNCs from bean seed hulls suggests great efficacy to recover the under-utilized agro-wastes thereby preventing air pollution.

Keywords: Bean seed hulls, Isolation, Cellulose nanocrystals, Cellulose triacetate, Characterization

1.0 INTRODUCTION

The inability of most African countries to follow the universal trend of waste recycling has increased the quantity of agricultural trash produced yearly. Burning and open dumping of agro-wastes are prevalent practices in Nigeria. This burning of agro-wastes decreases agricultural output, contributes to climate change, contributes to unfriendly and undesirable environment and causes respiratory illness such as bronchitis, eye irritation, asthma etc. On the other hand, many of these agro-wastes are allowed to rot away unused. For instance, bean seed husks is a biomass

that is carelessly dumped in different regions of Nigeria thereby resulting in environmental pollution [1-5]. The need to protect the environment from air pollution resulting from burning, open dumping or burying of agricultural wastes has led to the extraction of cellulose from these agro-wastes, which is economically and environmentally friendly. Thus, the trends of using agro-wastes and underused plants containing cellulosic fibres such as rice husks, rice straw, sugarcane bagasse, pineapple peels, bean seed husks, plantain stem, walnut shell, tomato peels, maize stem, maize cobs, corn fibres, cotton stalks, cotton seed hulls and burr, bamboo pulp, oil palm trees, saw dust from woods, raffia, wheat straw, wheat bran etc. are on the increase [6,1,7-10].

The demand for renewable and eco-friendly sustainable materials is ever-increasing and has tremendously increased the production of cellulose from agriculture biomass, marine animals, algae, protozoans, bacteria and fungi thereby making crop and animal wastes useful. Cellulose nanocrystals are referred to as second generation renewable resource. It also serve as a better replacement for the petroleum-based products. The major attention being given to nanocrystalline cellulose is on the increase because of its low density, great rigidity, great tensile strength, and high flexibility, renewable and biodegradable properties. Agricultural wastes biomass are of great importance because of the following reasons: it is environmentally friendly, it has low cost, it is readily available, it is renewable and it exhibits acceptable mechanical properties [11-14, 9].

Lignin, hemicellulose and cellulose are the most important components of plants. Lignin covers, encloses and protects hemicellulose and cellulose. Hemicellulose is a polysaccharide composed of xylose, glucose, arabinose, mannose and galactose [15]. Cellulose is one of the most important polysaccharides produced in plants from carbon (iv) oxide and water by the process of photosynthesis and are made up of glucose units linked by a β - 1,4 -glycosidic linkage with a regular network of intra and intermolecular hydrogen bonds [16-19]. Cellulose with the formula $(C_6H_{10}O_5)_n$ is the chief structural material of plant cell walls which gives the plant rigidity and form. It is likely the most prevalent organic material known [1, 20, 21]. Acid hydrolysis using H_2SO_4 or HCl process is mainly used for the isolation of cellulose nanocrystals (CNCs) from cellulose fibres present in different vegetable natural sources. Sulphuric acid hydrolysis introduces small number of sulphate ester groups into the surface of the CNCs making it easily dispersed in water whereas HCl hydrolysis leaves the surface chemistry of CNCs unchanged.

Cellulose nanocrystals have been generally considered as reinforcement segment in biodegradable plastic because of their biodegradability, easy accessibility, very crystalline form and capacity to enhance the qualities of bio composite[22, 23, 16, 24, 25]. Cellulose is the starting material for the production of cellulose triacetate. When the cellulose is treated with acetic anhydride or acetic acid in the presence of sulphuric acid, cellulose triacetate can be formed [20].

The aims of this study are to (i) isolate raw cellulose from bean seed husks and then convert it to CNCs (ii) convert the CNCs to cellulose triacetate (iii) determine some of the physical properties of both CNCs and CTA (iv) investigate the chemical characterization of both CNCs and CTA using Scanning electron microscopy (SEM), Fourier transform infrared (FTIR) and Gas chromatography-mass spectrometry (GC-MS) analyses (v) ascertain the effect of acetylation on the physico-chemical properties of CNCs.

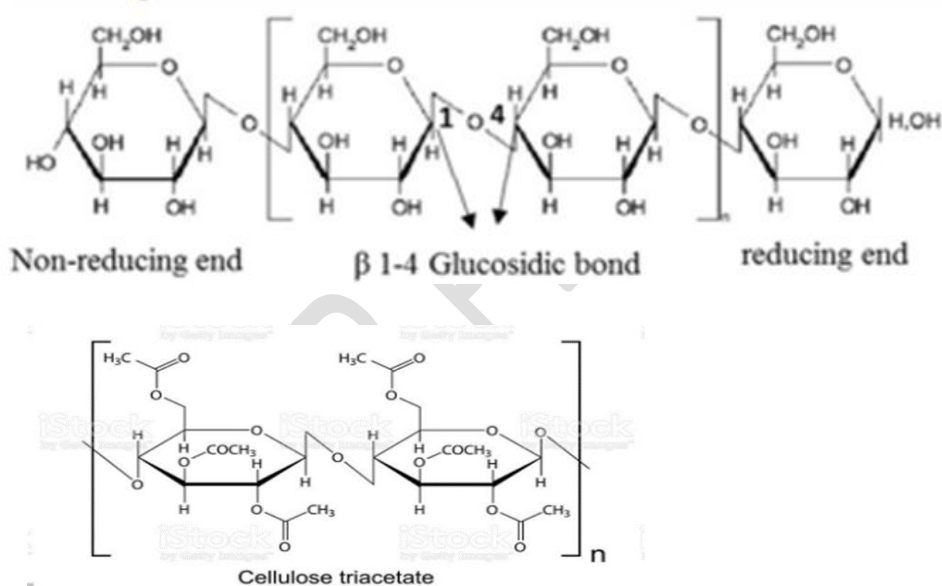


Fig. 1: Structural formulae of cellulose and cellulose triacetate

2.0 MATERIALS AND METHODOLOGY

2.1 COLLECTION AND PROCESSING OF SAMPLE

The beans hulls were gotten from Ubani main market in Umuahia North Local Government Area of Abia State, Nigeria and then ground with a grinding machine into fine particles and became ready for cellulose extraction.

2.2 MATERIALS

Conical flask, Weighing balance, Beaker, Oven, Masking Tape, Filter Paper, Foil, Measuring Cylinder, Spatula, Magnetic stirred heater, Crucible, pH meter, Pipette, glass centrifuge tubes, gooch crucible, Buck Scientific M530 USA FTIR, SEM Quanta FEG450(FEI)(APOLLOX-EDAX), Buck M910 Gas Chromatograph equipped with HP-5MS Column, shaking water bath, mechanical stirrer, test tubes, universal indicator, dropper, glass stirring rod, dessicator, Erlenmeyer flask, reflux condenser, petri dish, platinum crucible, muffle furnace, pycrometer, melting point apparatus.

2.3 REAGENTS

Ether, Ethanol, Distilled water, Sodium hydroxide (NaOH), Sulphuric acid (H₂SO₄), Sodium hypochlorite (NaOCl), Acetic anhydride, glacial acetic acid, 2-naphtol, Schweitzer's reagent, Conc. HCl, deionized water, conc. Nitric acid, nujol, benzene, potassium bromide (KBr), deuterated triglycerine sulphate.

2.4 METHODS

2.4.1 Alkali Treatment

5g of the ground sample was dissolved in 2w/v% NaOH in a solid to liquid ratio of 1g/10ml. The solution was then heated at 40⁰C for 45mins in a shaking water bath for 4hours. The alkali treatment was repeated 4 times until no more discoloration occurred. The sample solution was further washed with distilled water until pH 7 (neutral) was obtained and then the sample was oven dried at 60⁰C until a constant weight was obtained. The cellulose was hydrolysed with 2 w/v% NaOH for 15mins, 30mins and 45mins respectively at 40⁰C [6].

2.4.2 Bleaching Treatment

The essence of bleaching process is to remove lignin and other components so as to obtain purified cellulose. The sample resulting from the alkali treatment is blended with the bleaching agent sodium hypochlorite. 1g of sample to 50ml of bleaching agent solution is heated at 80⁰C,

shaken at 100rpm for 2hours using a shaking water bath and repeated two times to obtain a white product. The bleached sample was then thoroughly washed using distilled water until pH 7 to obtain white cellulose [6].

2.4.3 Sulphuric Acid Hydrolysis

Cellulose nanocrystals were then isolated from the white cellulose by acid hydrolysis through the treatment with 64 w/w% sulfuric acid solution at 50⁰C for 30mins, 60mins and 90mins respectively under constant mechanical stirring. This suspension was diluted 10-fold with cold deionized water to quench the hydrolysis reaction and then centrifuged to remove the excess acid. The resultant precipitate was washed several times by centrifugation with deionized water until a neutral pH was reached finally yielding the cellulose nanocrystals [26, 27].

2.4.4 Confirmatory Test for Cellulose

The best reagent for confirming cellulose is Schweitzer's reagent. CNCs was treated with the Schweizer's reagent (tetraammine copper (ii) hydroxide dihydrate). Cellulose was also treated with conc. HCl. Schweitzer's reagent is a deep blue solution prepared by dissolving copper (ii) hydroxide in excess of ammonia. It has a strong ammonia smell.

2.4.5 General Test for Carbohydrate

Molisch's Test: This is a general test for carbohydrates. 5mg of the cellulose nanocrystals was placed in a test tube containing 0.5ml of water and mixed with 2 drops of 10% solution of 2-naphtol in ethanol. 1ml of conc. sulphuric acid was pipetted into the solution, the acid formed a layer beneath the aqueous solution common surface of the liquids; the colour quickly changed on standing or shaking with a dark purple solution being formed. The mixture was shaken and allowed to stand for 2 minutes. A dull violet precipitate appeared [28].

$$\% \text{ Cellulose} = \frac{\text{mass of CNC obtained}}{\text{mass of initials sample}} \times \frac{100}{1}$$

2.4.6 Acetylation of Cellulose Nanocrystals;

Acetylation of cellulose nanocrystals using acetic anhydride or acetic acid in the presence of the catalyst H_2SO_4 gives the textile material named Cellulose triacetate. The three -OH groups of the cellulose were acetylated.

Procedure:

5g of the CNCs was dissolved in 10ml of glacial acetic acid and heated at $47.5^{\circ}C$ for 1 hour and 5ml of acetic anhydride added with 5.5 wt% sulfuric acid as catalyst. The mixture was further heated for 3 hours at the same temperature. After the completion of acetylation process, the acetylated cellulose was thoroughly washed to remove odour and any possible soluble impurities that may have accompanied the reaction process and it is then dried in an oven at $60^{\circ}C$ to constant weight [10].

$$\text{Weight percent gain (WPG)} = \frac{W_{\text{final}} - W_{\text{initial}}}{W_{\text{initial}}} \times \frac{100}{1}$$

Where, W_{final} = weight of oven dried acetylated CNC

W_{initial} = weight of CNC before acetylation

2.4.7 Procedure for Solubility Tests

a) Solubility in water

0.10g portion of the cellulose nanocrystals or cellulose triacetate in a small test tube (100 x 12mm) was treated with successive 1.0ml portion of H_2O shaking vigorously after each addition, until 3.0ml was added. If the cellulose does not dissolve completely in 3.0ml of H_2O , it may be regarded as insoluble in water. The content of the small test tube was tested with universal indicator paper, a little of the solution or supernatant liquid was removed with a dropper [28].

b) Solubility in ether

0.10g of the solid cellulose nanocrystals or cellulose triacetate in a dry small test tube was treated with successive 1.0ml portions of ether, shaking vigorously after each addition, until 3.0ml of ether was added. More than 3ml of ether shouldn't be employed [28].

c) Solubility in ethanol

0.10g of the solid cellulose nanocrystals or cellulose triacetate in a dry small test tube was reacted with successive 1.0ml portions of ethanol shaking vigorously after each addition until 3.0ml of ethanol was completely added [28].

2.4.8 Determination of Cellulose Content

Raw cellulose content was measured according to **ASTM, 2017**. 0.3g of sample was weighed into 50ml glass centrifuge tubes containing 50ml of water, centrifuged at 1500rpm for 10mins, and the supernatant decanted. The sample was resuspended in 12.5ml glacial acetic and 2.5ml of concentrated nitric acid and digested in a boiling water bath for 20min and the supernatant collected. The supernatant was transferred to a Gooch crucible (W_1), washed successfully with hot alcohol, 10ml of 90% benzene, and 60% of ether, dried and weighed, (W_3) finally ashed (W_2) and reweighed[29].

$$\text{Cellulose content} = \frac{W_3 - W_2}{W_1} \times 100$$

W_3 = weight of dried sample

W_2 = weight of ash content

W_1 = weight of sample

2.4.9 Lignin content Determination

0.3 ± 0.01g prepared sample was weighed to the nearest 0.1 mg and placed in a 16 x 100mm test tube. The initial sample weight was recorded as W_1 . Each sample was run in duplicate, at minimum. Samples for total solids determination (LAP-001) were weighed out at the same time as the sample for the acid – insoluble lignin determination. If this is done later, it can introduce an error in the calculation because ground biomass can rapidly gain or loss moisture when exposed to the atmosphere. The average total solids values were recorded as T_{final} . 3.00 ± 0.01ml (4.92 ± 0.01 g) of 72% H_2SO_4 was added and a glass stirring rod used to mix for 1 minutes, or until the sample is thoroughly wetted. The test tube was placed in the water bath controlled to 30 ± 1°C and hydrolyzed for 2 hours and then cooled in a desiccator and the weight, W_2 i.e the weights of the crucible, acid-insoluble lignin, and acid-insoluble ash were recorded to the nearest 0.1mg[29].

Calculation % acid – insoluble residue on an extractives – free basis as follows:

$$\% \text{ acid – insoluble residue} = \frac{W_2 - W_3}{W_1 \times \% T_{\text{final}}} \times 100\%$$
$$100\%$$

Where:

W_1 = initial weight of extracted sample

W_2 = weight of crucible, acid-insoluble residue, acid-insoluble ash

W_3 = weight of crucible and acid-insoluble ash

% T_{final} = % total solids of the extracted sample determined at 105⁰C as described by the standard method for the determination of total solids in biomass.

2.4.10 Hemicellulose Determination

Hemicelluloses content was measured according to **ASTM, 2017**. 1g of sample was weighed and placed in a 20 x 150mm test tube and recorded as W_1 , the initial sample weight. 15ml of 72% was added and stirred for 1minute until the sample was thoroughly wetted. The sample was transferred to a 1000ml Erlenmeyer flask and diluted to 500ml with deionized water. The flask was then placed on the heating manifold and attached to the reflux condenser, gently boiled and refluxed for 4 hours. At the end of 4 hours, the condenser was rinsed with a small amount of deionized water before disassembling reflux apparatus. The hydrolyzed solution was placed on the crucibles. The weight of collected filtrate was measured. The crucible and contents was dried at 105±30⁰C for 2 hours and then cooled in dessicators and recorded as W_2 . The weight of the crucible, and contents were placed in the muffle furnace and ignited at 575⁰C for a minimum of 3 hours, or until all the carbon is eliminated. Then it was cooled in dessicators and recorded as W_3 [29].

Note: total solid = 100 – moisture content

Calculations

$$\% \text{ Hemicellulose} = \frac{(W_2 - W_3)}{W_1 \times [\% T_{\text{final}}]} \times 100$$

100%

Where W_1 = initial sample weight.

W_2 = weight of crucible and dried content

W_3 = weight of crucible and contents minus carbon

2.4.11 Moisture Content Determination

A petri-dish was washed and dried in the oven. Approximately 1-2g of the sample was weighed into petri dish. The weight of the petri dish and sample was noted before drying. The petridish and sample were put in the oven and heated at 105⁰C for 2hr with the result noted and heated another 1hr until a steady result was obtained and the weight was noted. The drying procedure was continued until a constant weight was obtained[29].

$$\% \text{ Moisture content} = \frac{W_1 - W_2}{\text{Weight of sample}} \times 100$$

Where W_1 = weight of petridish and sample before drying

W_2 = weight of petridish and sample after drying.

2.4.12 Ash content Determination

AOAC, 2017 method was used. Empty platinum crucible was washed, dried and the weight was noted. Approximately 1- 2g of sample was weighed into the platinum crucible and placed in a muffle furnace at 550⁰C for 3 hours. The sample was cooled in a dessicator after burning and weighed[30].

Calculations:

$$\% \text{ Ash content} = \frac{W_3 - W_1}{W_2 - W_1} \times 100$$

Where

W_1 = weight of empty platinum crucible

W_2 = weight of platinum crucible and sample before burning

W_3 = weight of platinum and ash.

2.4.13 Direct pH Determination

A small quantity of the sample was dissolved in water or another solvent, and the pH of the resulting solution was measured using a pH meter [31].

2.4.14 Density Determination

Pycnometer method: A small, calibrated glass container (pycnometer) was filled with a known volume of liquid and weighed. The pycnometer was then emptied and filled with the sample, and the weight measured again. The difference in weight between the two measurements was used to calculate the volume of the sample, which was then used to determine the density [29].

2.4.15 Melting Point Determination

The capillary tube containing the sample was inserted into a slot behind the viewfinder of a melting point apparatus. There are usually three slots in each apparatus, and multiple melting points was taken simultaneously. The apparatus was turned on and the setting adjusted to an appropriate heating rate. The rate of heating is often experimental and was adjusted by careful monitoring of the thermometer on the apparatus. A magnified view of the illuminated sample in the apparatus was seen by looking through the viewfinder. The sample was heated at a medium rate to 20°C below the expected melting point, then the rate of heating slowed such that the temperature increases by not more than 1°C every 30 seconds (i.e., very slowly). The process was repeated with a fresh sample after allowing the apparatus to cool and the recommendations for compound with known expected melting point was used to perform a more careful assessment of the melting point[29].

2.5 INSTRUMENTAL ANALYSIS

2.5.1 Procedure for FTIR

Buck scientific M530 USA FTIR was used for the analysis. This instrument was equipped with a detector of deuterated triglycine sulphate and beam splitter of potassium bromide. The software of the Gram A1 was used to obtain the spectra and to manipulate them. An approximately of 1.0g of samples, 0.5ml of nujol was added, they were mixed properly and placed on the salt pellet. During measurement, FTIR spectra was obtained at frequency regions of 4,000– 600 cm^{-1} and co-added at 32 scans and at 4 cm^{-1} resolution. FTIR spectra were displayed as transmitter values.

2.5.2 Scanning electron microscope

Morphological investigations of the composite particles were carried out with SEM Quanta FEG 450 (FEI) (APOLLO X - EDAX), U.S.A. 0.5g Samples were coated with Au/Pd film and the SEM images were obtained using a secondary electron detector. Point chemical analysis was performed in 2 independently selected particles.

2.5.3 Quantification by GC-MS

The analysis of phytochemical was performed on a BUCK M910 U.S.A Gas chromatography equipped with HP-5MS column (30 m in length \times 250 μ m in diameter \times 0.25 μ m in thickness of film). Spectroscopic detection by GC–MS involved an electron ionization system which utilized high energy electrons (70 eV). Pure helium gas (99.995%) was used as the carrier gas with flow rate of 1 ml/min. The initial temperature was set at 50–150 °C with increasing rate of 3 °C/min and holding time of about 10 min. Finally, the temperature was increased to 300 °C at 10 °C/min. One microliter of the prepared 1% of the extracts diluted with respective solvents was injected in a splitless mode. Relative quantity of the chemical compounds present in each of the extracts of was expressed as percentage based on peak area produced in the chromatogram.

2.6 STATISTICAL ANALYSIS

The physical characterization were carried out in duplicates, and then the mean determined followed by subjection to standard deviation using Microsoft excel 2010 package. The weight percent gain plots were done using the statistical software named Origin Pro graphing and analysis 2021.

3.0 RESULTS AND DISCUSSION

3.1 Physical properties

Cellulose nanocrystals dissolved in both schweitzer's reagent and conc. HCl confirming its presence. CNCs gave a positive test for carbohydrate. **Table 1** shows the data for the solubility test of CNCs and CTA in the solvents such as ethanol, water and ether. It is observed that cellulose nanocrystals is sparingly soluble in ethanol while the acetylated cellulose nanocrystals is completely soluble in ethanol. Out of the three solvents, ether was the best which dissolved both CNCs and CTA. From **Table 2**, the chemical content of the raw ground bean seed hulls

were in the order cellulose (27.333%) > lignin (10.918%) > hemicellulose (6.034%) > ash content (8.170%) indicating that cellulose is the main component of plant cell walls which gives plant rigidity and form. From **Table 3**, CTA has a higher melting point (228.31⁰C) than cellulose nanocrystals (142.50⁰C). The density of CNCs (1.1005g/ml) is slightly higher than that of CTA (0.90 g/ml). Both the densities of CNCs and CTA are approximately equal to the density of water (1.00g/ml) indicating that the particles of CNCs and CTA will form suspensions in water. The pH of CNCs is neutral (7.00) indicating that [H⁺] = [OH⁻] whereas the pH of CTA is very slightly acidic (6.59) showing that [H⁺] > [OH⁻] [32]. CNCs gave an extremely higher yield (42.31%) than CTA (3.28%). The moisture content in both CNCs (6.35%) and CTA (2.90%) were very low showing that it will be difficult for micro-organisms to break them down and therefore they could be stored for a long time without adding preservatives [33,34].

Table 1: Solubility Data

Compound	Solvent		
	Water	Ethanol	Ether
CNCs	Sparingly soluble	Insoluble	Sparingly soluble
CTA	Sparingly soluble	Insoluble	Completely soluble

Solubility test was run five times for each compound

Table 2: Chemical composition of raw bean seed hulls

Component	% Yield
Hemicellulose	6.034
Ash content	8.170
Lignin	10.918
Cellulose	27.333

Table 3: Physical characterization of CNCs and CTA from bean seed hulls

Parameter	CNCs	CTA
% Yield	42.31 ± 0.156	3.28 ± 0.106

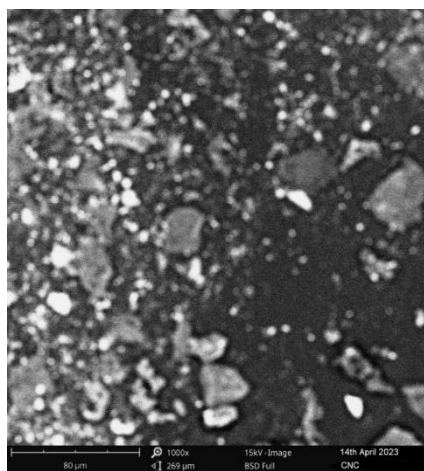
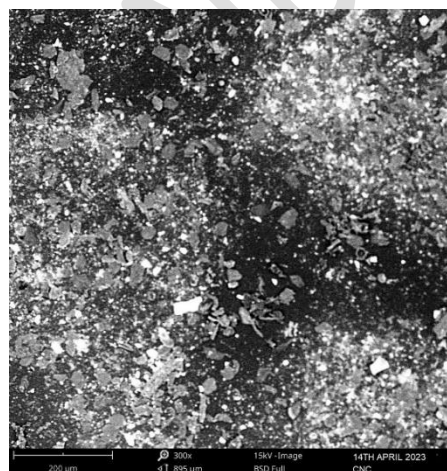
% Moisture	6.35 ± 0.212	2.90 ± 0.940
pH	7.00 ± 0.141	6.59 ± 0.014
Density (g/ml)	1.1005 ± 0.002	0.90 ± 0.003
Melting point ($^{\circ}\text{C}$)	142.50 ± 3.536	228.31 ± 0.014

Data reported as mean of duplicate determinations \pm standard deviation

x

3.2 Morphological analysis

The microscopic morphology of samples was observed using SEM. The SEM image of CNCs were observed under magnifications of 300x, 500x, 750x and 1000x respectively at a voltage of 15kV (**Fig.2**). CNCs exhibited a rough surface and irregular fragments with disordered large surface area. The pores were well developed indicating that CNCs can serve as a good adsorbent [35, 36]. Acetylation greatly influenced the morphology of CNCs. The SEM micrograph of CTA was taken at the voltage of 10kV under magnifications of 300x, 500x, 1000x and 1500x respectively as depicted in **Fig.3**. The amount of the fragments and pore sizes in CTA were greatly reduced with very small surface area. As a result, CTA will not be an effective adsorbent when compared to CNCs [37, 38]. There was reconfiguration of the disordered fragments into a very few ordered particles in CTA. The interfacial space among the fragmented particles were very narrow in CNCs but extremely wide in CTA. From the scanned image, the pore sizes of the fragmented particles in both CNCs and CTA decreased with increasing magnification. The porosity of CNCs were greatly higher than that of CTA making it a better adsorbent than CTA [39, 40].



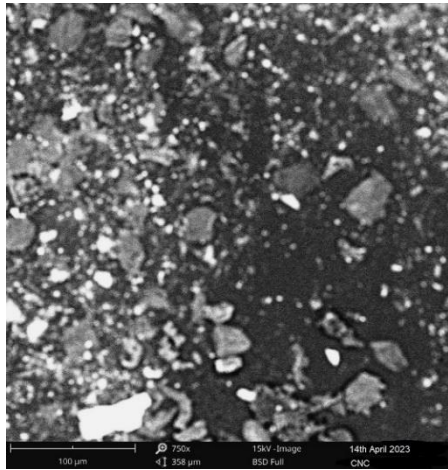
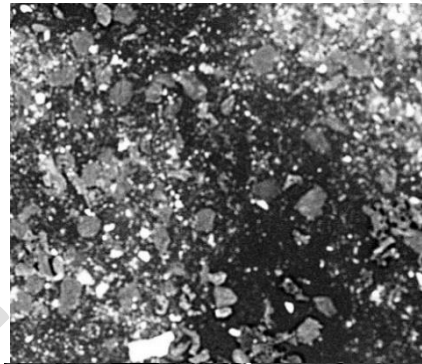
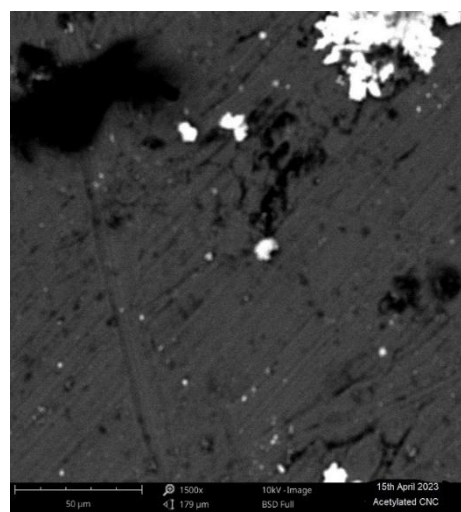
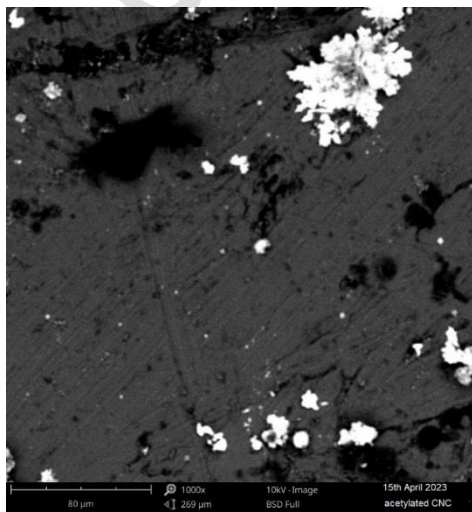
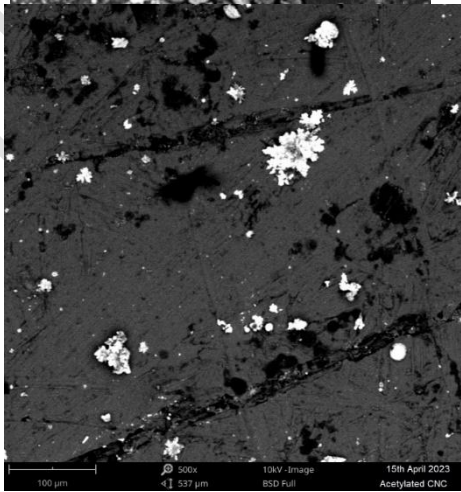
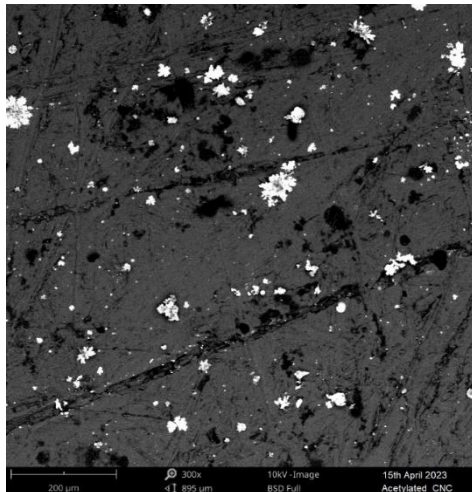


Fig. 2: SEM images of cellulose alkali treated and bleached bean seed



nanocrystals from hulls



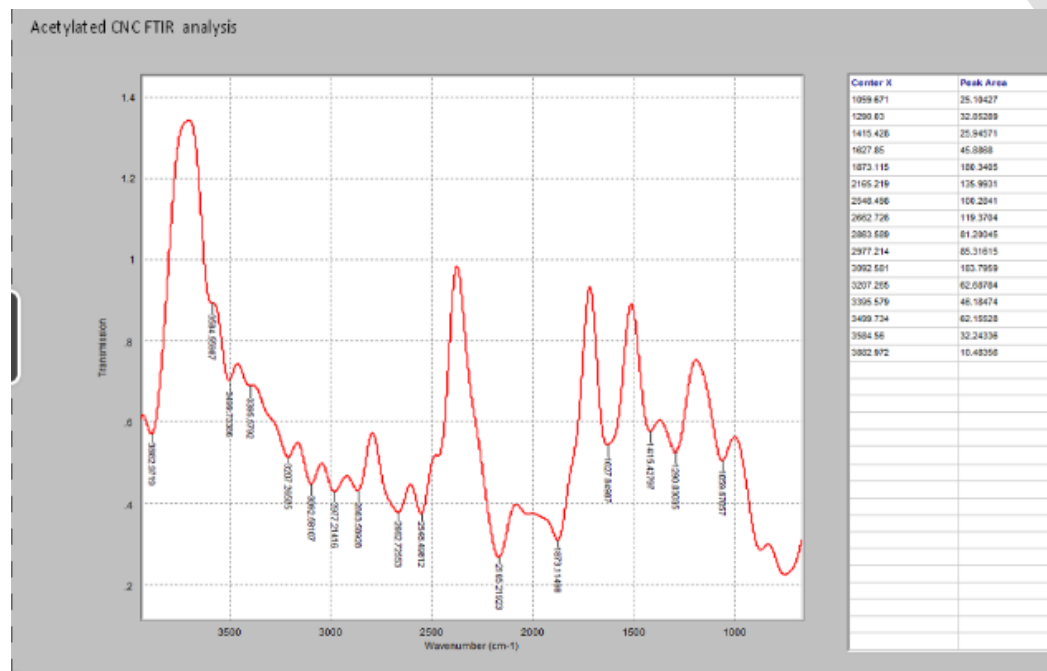


Fig. 3: SEM images of Cellulose triacetate

3.3 FTIR Analysis

The structures of CNCs and CTA samples were analysed using FTIR (**Fig. 4**). The bands observed in both spectra are strongly associated with the structures of cellulose, cellulose triacetate, hemicellulose, pectin, wax and lignin, suggesting that lignin and hemicellulose contents in the sample were not completely removed by the pre-treatment process.

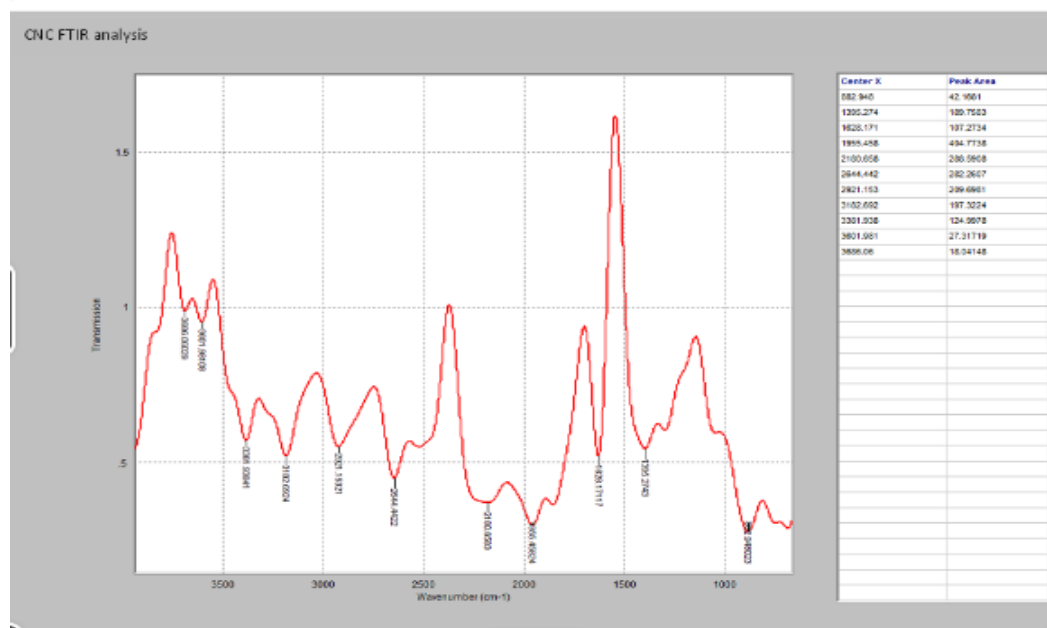


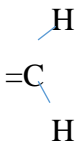
Fig. 4: FTIR Spectra of CNCs and CTA

Table 4: FTIR Spectra Results for CNCs extracted bean seed hulls

Frequency (cm ⁻¹)	Functional group
882.948	N-H out-of-plane bend of amines In-plane, out-of-plane wagging vibrations of adjacent hydrogens of meta-substituted benzenes
1395.274	C-O stretch of esters, carboxylic acids O-H bend of alcohols
1628.171	C=C of non-conjugated alkenes C=O stretch of tertiary amide
1955.458	C=C=C Stretch of allenes
2180.658	[O-C≡N] ⁻ of cyanates, C≡N ⁻ of cyanides, [SC≡N] ⁻ of thiocyanates C≡C stretch of alkynes
2644.442	Hydrogen-bonded O-H stretch of carboxylic acids
2921.153	Hydrogen bonded O-H stretch of carboxylic acids C-H stretch of alkanes
3182.692	Intra-molecular H-bonded O-H of alcohols N-H stretch of primary amide
3381.938	N-H stretch of primary aromatic amine N-H stretch of primary amide
3601.981	Free O-H stretch of alcohols and phenols
3686.06	Free O-H stretch of alcohols and phenols

Table 5: FTIR Spectral Results for Cellulose triacetate

Frequency (cm ⁻¹)	Functional group
1059.671	C-O stretch of alcohols S=O stretch of sulphur compounds

1290.03	C-N stretch of aromatic amines C=O stretch for esters
1415.428	O-H in-plane bend of carboxylic acids In-plane bending of unsaturated C-H bond of 
1627.85	N-H in plane bend of primary amine C=C stretch of alkenes Free C=O stretch of tertiary amide
1873.115	C=O stretch of acid anhydride
2165.219	[O-C≡N] ⁻ of cyanates, C≡N ⁻ of cyanides, [SC≡N] ⁻ of thiocyanates C≡C stretch of alkynes
2548.496	Hydrogen bonded O-H of carboxylic acids
2662.726	Hydrogen bonded O-H of carboxylic acids
2863.589	C-H stretch of alkanes
2977.214	C-H stretch alkanes Intra-molecular H-bonded O-H of alcohols in chelate form
3092.581	=C-H of alkenes
3207.265	Hydrogen bonded O-H of alcohols
3395.579	N-H stretch of primary aromatic amine
3499.734	N-H stretch of primary aliphatic amine
3584.56	Free O-H stretch of alcohols and phenols
3882.972	Free O-H stretch of alcohols and phenols

Considering **fig. 4**, **table 4** and **table 5**, methyl and methylene groups both have asymmetric and symmetric C-H stretching vibration modes, giving rise to four absorption bands just below 3000cm^{-1} . The presence of a small sharp band just above 3000cm^{-1} is due to unsaturated =C-H stretching vibration of alkenes. The in-plane bending vibration (or scissoring) of the C-H bond in =CH₂ group produces a band near 1415cm^{-1} . The adsorption in the $1420\text{-}1290\text{cm}^{-1}$ region with weak intensity is as a result of in-plane bending of the unsaturated C-H bond. The C=C

stretching vibration gives rise to an absorption band in the $1680\text{-}1620\text{cm}^{-1}$ region in simple alkenes; the band is of variable intensity but is much less intense than that from the $\text{C}=\text{O}$ stretching vibration which also leads to absorption in this region. Conjugated double bonds of aliphatic systems such as dienes, trienes and tetraenes show two, three and four bands respectively in the $1650\text{-}1600\text{cm}^{-1}$ region [28]. The $\text{C}\equiv\text{C}$ stretching vibration gives rise to a weak absorption in the $2260\text{-}2100\text{cm}^{-1}$ region of the spectrum with variable intensity [28, 41]. Free O-H stretching band for alcohols and phenols is in the $3650\text{-}3590\text{cm}^{-1}$ region. O-H band recognised as strong broad band in the $3400\text{-}3200\text{cm}^{-1}$ region is due to intermolecular hydrogen bonding which results in the weakening of the O-H bond; thus, broadening and shifting to lower frequency. Hydrogen bonded O-H of carboxylic acids show absorption in the region $3300\text{-}2500\text{cm}^{-1}$ with very broad band [32, 28, 41]. The band at 1060cm^{-1} is characteristics of C-O stretch for primary alcohols. The C-O stretching vibrations in esters give rise to very strong bands in $1300\text{-}1100\text{cm}^{-1}$ [28, 32]. Allenes show a moderately intense band (sometimes as a double peak) at $2000\text{-}1900\text{cm}^{-1}$ due to the asymmetric $\text{C}=\text{C}=\text{C}$ stretching vibrations [28, 41]. In dilute solutions, primary amines give two absorption bands, one near 3500cm^{-1} and the other near 3400cm^{-1} arising from the asymmetric and symmetric stretching vibrations of the two N-H bonds. The N-H out of plane bending of amines within the absorption range of $910\text{-}660\text{cm}^{-1}$ [28, 41, 32]. All acid anhydrides show two strong absorption bands of C=O stretch near 1800cm^{-1} and 1750cm^{-1} , and they are almost always 60cm^{-1} apart [28, 41]. C-O stretch and O-H in-plane deformation vibrations of carboxyl groups absorb at $1440\text{-}1395\text{cm}^{-1}$ (weak). The C-O stretching vibration in esters give rise to very strong bands in $1300\text{-}1100\text{cm}^{-1}$ region [28,41]. C=O stretch of tertiary amide in dilute solution absorb at $1670\text{-}1630\text{cm}^{-1}$ region with strong band [32]. C-N stretch of aromatic amine absorption band falls in the range $1340\text{-}1260\text{cm}^{-1}$ [32]. The in-phase, out-of-plane, wagging vibrations of adjacent hydrogens of substituted benzenes give rise to strong absorption in well-defined frequency ranges in the $900\text{-}690\text{cm}^{-1}$ region of the spectrum [28, 41]. The adsorption pattern with meta-substituted benzenes give rise to two apparent bands, one at $810\text{-}750\text{cm}^{-1}$ and the other at $900\text{-}860\text{cm}^{-1}$ [28, 41]. S=O stretch of sulphur compounds absorbs in the region of $1060\text{-}1040\text{cm}^{-1}$ with strong band [28, 41]. Inorganic ions such as cyanide, thiocyanate and cyanate absorb in the region of $2200\text{-}2000\text{cm}^{-1}$ [41].

3.4 GC-MS Analysis

Gas chromatography mass spectrometry is used to determine the chemical composition of the CNC and its derivative cellulose triacetate. The GC-MS results of cellulose nanocrystals (**Fig. 5 and Table 6**) revealed the presence of organic compounds such as aliphatic hydrocarbons, phenolic compounds, saturated aliphatic carboxylic acids, aliphatic halogenocarboxylic acid, unsaturated aliphatic hydrocarbons, aliphatic ketones, aromatic ketone, diene, phthalate esters, aromatic alcohol, thiol, fatty acids, unsaturated aliphatic carboxylic acid, alkane sulphonyl chloride, triterpene, steroid, esters, aromatic alcohol, organometalloid compounds and amine [28]. On the other hand, the GC-MS results of cellulose triacetate (**Fig.6 and Table 7**) disclosed the presence of organic compounds such as saturated aliphatic hydrocarbons, unsaturated aliphatic hydrocarbons, aliphatic alcohols, saturated halogeno aliphatic compound, aliphatic ketone, phthalate esters, aliphatic carboxylic acid, aliphatic halogenocarboxylic acid, esters and triterpene [28].

Squalene, a triterpene present in CNCs has anti-cancer activity especially the tumour growth around blood vessels [42]. Amines are used as painkillers, as anaesthetic, as solvents in Benadryl syrups, regulates vitamin levels in the body and serves as useful stimulants for neurotransmitters like serotonin for our bodies [43]. Carboxylic acids are used as solubilizer for antibiotic or antihistamine drug, as antihypertensive drugs, as blood cholesterol reducing drugs, as nonsteroidal anti-inflammatory drugs and as analgesics [44,45]. Thiol containing drugs are used as chelators of heavy metal ions, removing them from blocking enzyme activity in the body and promoting oxidation; they serve as antioxidants in the body i.e prevents the oxidation of protein, lipids and DNA in the body [46]. Ketones are used in chemical peeling and for acne treatments; ketones maintain brain function in the absence of glucose; enter the bloodstream and are used by the heart, kidney and skeletal muscle [47]. Phenols act as antioxidants and prevents cancer but can be toxic in high amounts; relieves symptoms caused by sore throat, used as preservatives in vaccines; phenol-based products are used as oral analgesics; used to treat tight muscles [48]. Phenolic compounds exhibits various biological activities such as antimicrobial, anti-inflammatory and antioxidant properties [49, 50]. Dihydroxy isosteviol methylester with the highest percentage composition of 26.58% is capable of inducing apoptosis in cancer cells signifying its utilization in drug design for chemoprevention [51]. Phthalates are converted to metabolites in the body which is excreted in urine, faeces and sweats. In human, phthalates cause type II diabetes, insulin resistance, overweight /obesity, allergy, asthma, higher systolic blood

pressure, low birth weight, earlier menopause, pregnancy loss, preterm birth. Some phthalate metabolites were negatively associated with breast cancer, increased risk of thyroid cancer in children, toxicity on genetal development; determines semen quality and precocious puberty in male children [52]. Steroids are anti-inflammatory drug used to treat rheumatoid arthritis, lupus or vasculitis (inflammation of the blood vessels) [53]. Halogenated aliphatic and aromatic hydrocarbons are known to exhibit high activity against different nematodes and trematodes parasitizing domestic animals and humans [54]. Fatty acids are used as a vehicle and lubricant in pharmaceutical preparations; it have been used extensively as an additive for development of nanodrug delivery systems [55]. Aliphatic hydrocarbons are used in extraction processes in pharmaceuticals; they are axphysiants and central nervous system depressants. Many paraffins cause chemical pneumonitis [56]. Aliphatic and aromatic alcohols are used as antiseptic, disinfectant and antidote; used as a solvent and intermediate in the pharmaceutical industries; used in human medicine as an anti-microbial preservative and as a local anesthetic and antipruritic. Aliphatic alcohols show increasing potency as non-selective central nervous system depressants [57]. Conjugated dienes demonstrates antifungal and antibacterial properties [58,59].

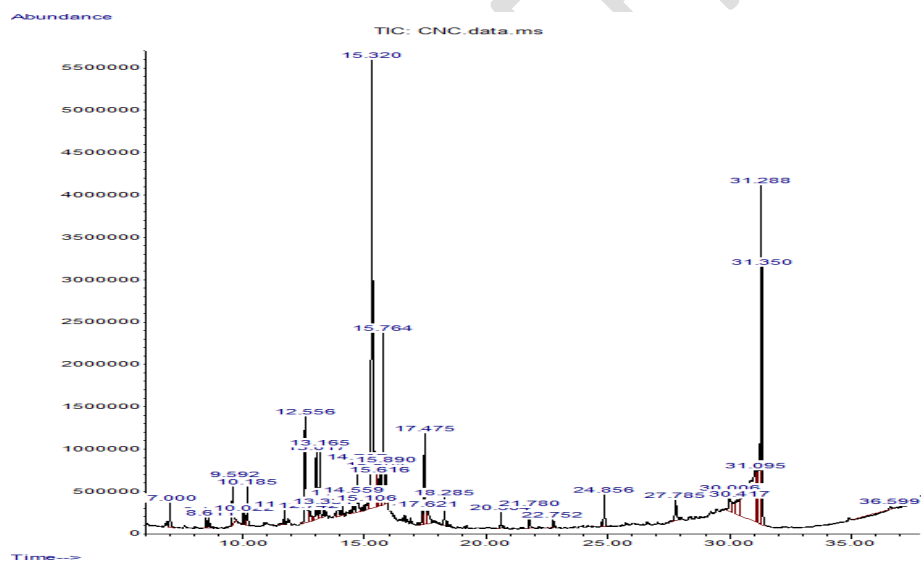

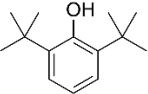


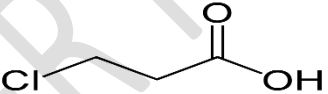


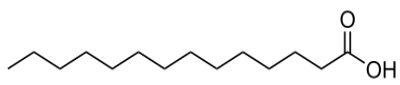
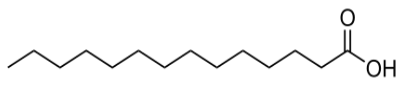
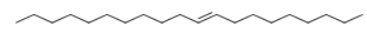
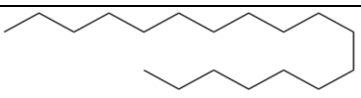

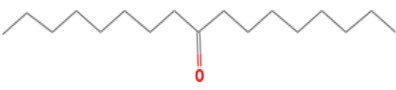
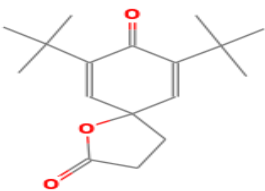

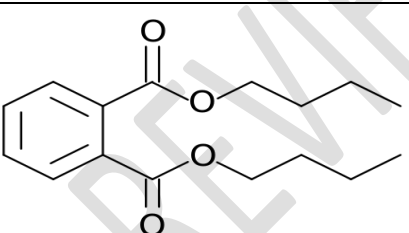
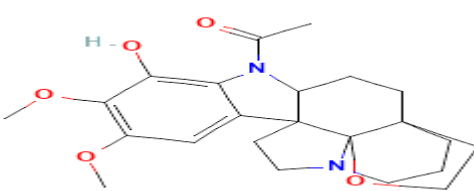
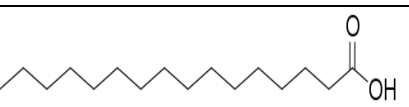
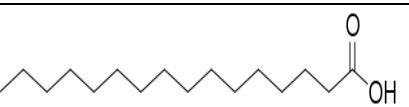
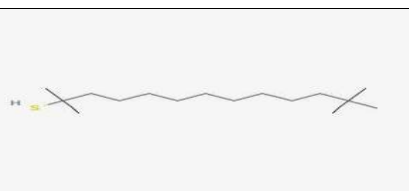


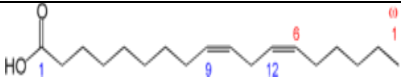
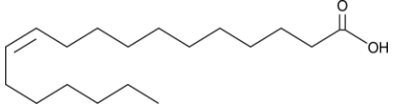
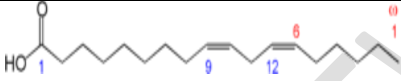


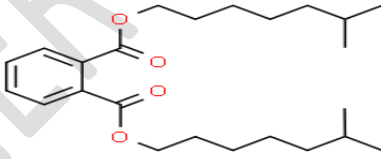


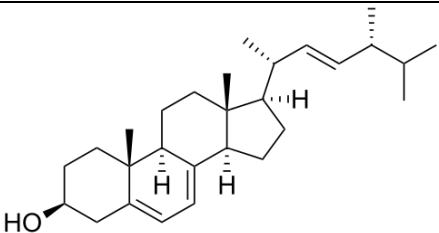
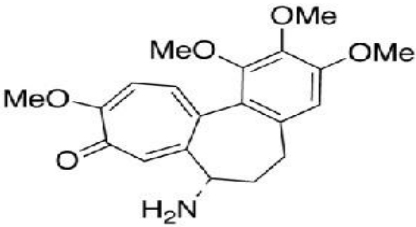
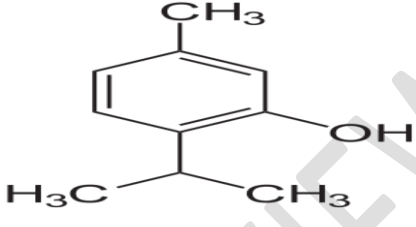
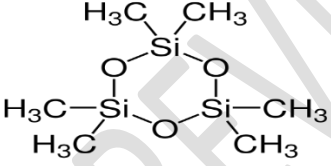
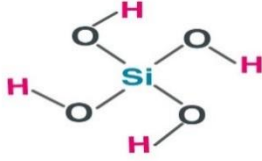
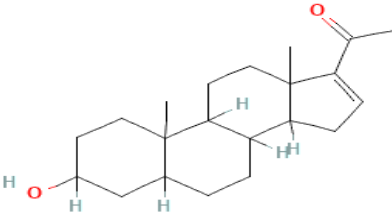
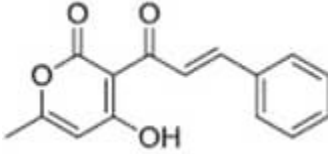


Fig 5: GC-MS spectra for CNCs

PEAK	RETENTION TIME	COMPOUND NAME	STRUCTURE	% AREA
1	7.00	Tetradecane		0.88
2	8.481	2,4-tert-butylphenol		0.46
3	8.611	Pentadecane		0.35
4	9.592	Dodecanoic acid		1.87
5	10.022	3-chloropropionic acid		0.34
6	10.185	Hexadecane		1.11
7	11.706	Heptadecane		0.50
8	12.556	Tetradecanoic acid		5.07
9	12.742	Tetradecanoic acid		0.62
10	13.017	9-Eicosene		2.24
11	13.165	Octadecane		2.18
12	13.331	1-octadecanesulphonyl chloride		0.49

13	13.920	9-Heptadecanone		0.94
14	14.062	7,9-Di-tert-butyl-1-oxaspiro (4,5)deca-6,9-diene		0.65
15	14.559	Nonadecane		0.74
16	14.707	Dibutyl phthalate		2.03
17	15.106	Aspidospermidin-17-ol		0.47
18	15.320	n-Hexadecanoic acid		23.43
19	15.504	n-Hexadecanoic acid		1.68
20	15.616	tert-Hexadecanethiol		1.70
21	15.764	1-Docosene		5.64

22	15.890	Heptadecane		1.14
23	17.367	9,12-Octadecadienoic acid		0.61
24	17.475	Cis-Vaccenic acid		4.15
25	17.621	9,12-Octadecadienoic acid		0.95
26	18.285	1-Docosene		0.87
27	20.604	Pentadecafluorooctanoic acid		0.47
28	21.780	Diisooctyl phthalate		0.72
29	22.752	17-pentatriacontene		0.16
30	24.856	Squalene		1.13
31	27.785	Ergosterol		1.22

32	30.006	N-Acetoacetyl-deacetylcolchicine		1.52
33	30.417	Thymol		2.27
34	31.052	Cyclotrisiloxane		13.73
35	31.095	Silicic acid		1.82
36	31.288	16-pregnenolone		11.30
37	31.350	3-(3,4-dimethoxycinnamoyl)-4-hydroxy-6-methyl-2H-pyran-2-one		5.59

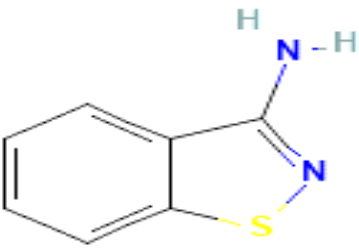
38	36.599	1,2-Benzisothiazol-3-amine	 <p>The image shows the chemical structure of 1,2-Benzisothiazol-3-amine. It consists of a benzene ring fused to a five-membered isothiazole ring. The isothiazole ring has a sulfur atom (S) at the bottom position and two nitrogen atoms (N) at the 1 and 2 positions. An amino group (-NH₂) is attached to the 3-position of the isothiazole ring. The nitrogen atoms and the amino group are highlighted in blue, and the sulfur atom is highlighted in yellow.</p>	-1.04
----	--------	----------------------------	---	-------

Table 6: GC-MS composition of CNCs

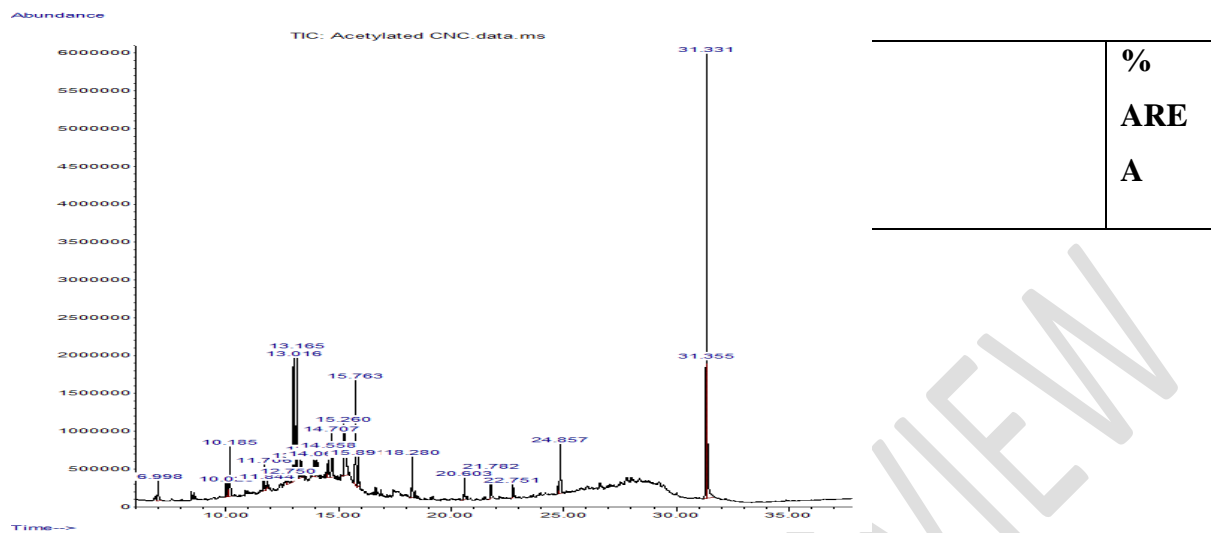







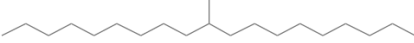

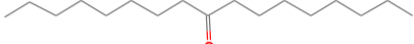


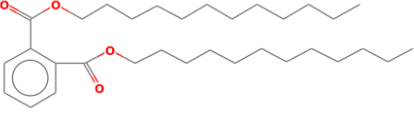





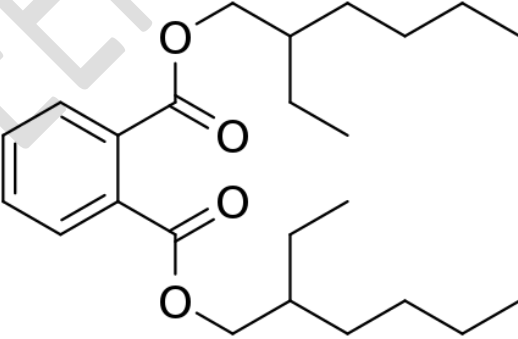
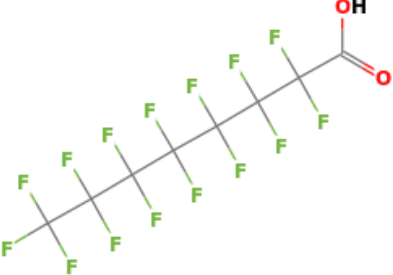


Fig. 6: GC-MS Spectra of CTA

1	6.99	Tetradecane		1.81
2	10.025	5-tetradecene		1.14
3	10.185	Hexadecane		3.82
4	11.706	Heptadecane		1.86
5	11.844	Dodecane		0.55
6	12.750	1-decanol		0.80
7	13.016	1-octadecene		9.76
8	13.165	10- methyl nonadecane		9.87
9	13.328	1- chloroeicosane		2.12
10	13.925	9- heptadecanone		2.95
11	14.060	Cetene		1.62
12	14.558	Teratetraconta ne		2.27

13	14.707	Didodecyl phthalate		4.62
14	15.260	n-Hexadecanoic acid		7.64
15	15.763	1-octadecene		8.01
16	15.891	Octadecane		1.96
17	18.280	1-Docosene		2.95
18	20.603	1-Docosene		1.68
19	21.782	Bis (2-ethylhexyl) phthalate		2.27
20	22.751	Pentadecafluorooctanoic acid	 B	0.98

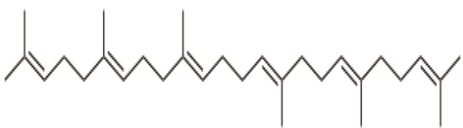
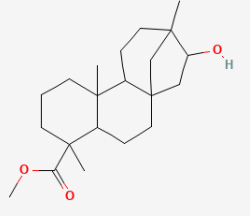
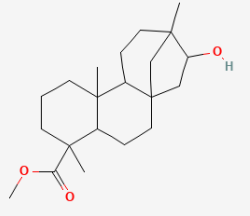
21	Aq12ws ezAFG	Squalene		4.73
22	31.331	Methyl dihydro isosteviol		15.39
23	31.355	Methyl dihydro isosteviol		11.19

Table 7: GC-MS composition of CTA

3.5 Weight percent gain (WPG)

Figures 7, 8, and 9 show the plots of WPG over reaction time, catalyst concentration and temperature of the acetylation of CNCs. The WPG of acetylated cellulose fluctuated with reaction time increment as well as with the fluctuation of catalyst concentration. The temperature of acetylation fluctuated alongside with the fluctuation of WPG. As the concentration of catalyst increased, both the temperature of acetylation and WPG fluctuated. **Table 8** displayed that the WPG was least (29.87%) at the highest temperature (60⁰C) but highest (72.22%) at mid temperature of 47.50⁰C suggesting that the decrease in temperature increased the WPG. At constant concentration of catalyst (5.50 wt%), the WPG fluctuated while the temperature became constant (47.5⁰C). Therefore, WPG was inversely proportional to temperature but varied with the concentration of catalyst. The reduction in WPG with increase in temperature was as a result of degradation of carbohydrate cellulose under the condition of strong acid and high temperature [10, 60, 61].

Table 8: Weight percent gain (WPG) of acetylated cellulose

Run	Time (hours)	Conc. of H ₂ SO ₄ (wt%)	Temp (°C)	WPG (%)
1	2.50	5.50	47.50	72.22
2	4.00	1.00	35.00	64.44
3	1.00	10.00	60.00	29.87
4	0.02	5.50	47.50	65.63
5	5.02	5.50	47.50	46.05

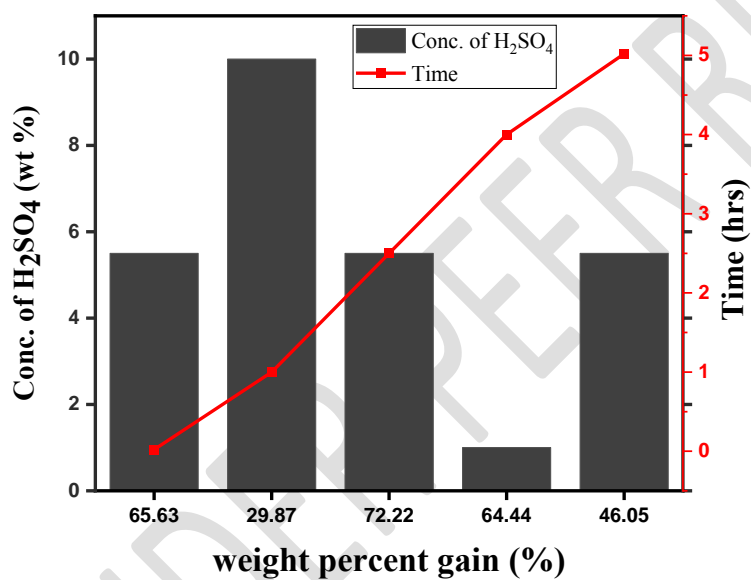


Fig. 7: Plot of WPG of acetylated cellulose as a function of catalyst concentration and reaction time

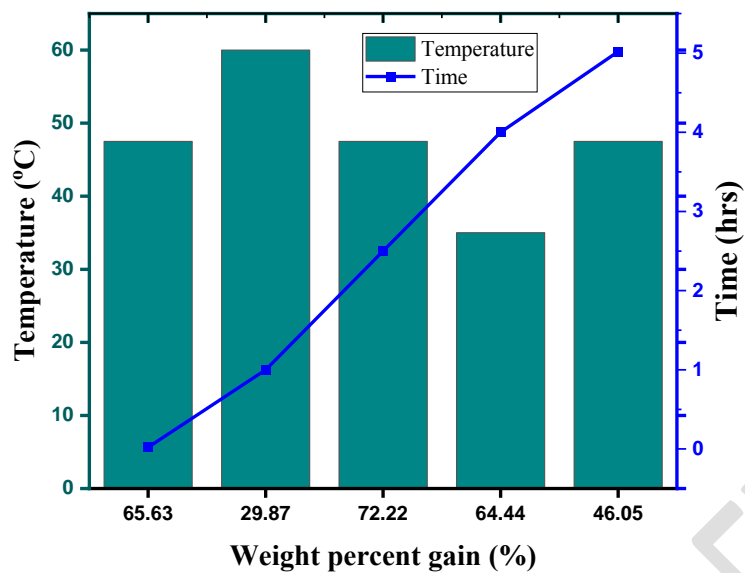


Fig. 8: Plot of WPG of acetylated cellulose as a function of temperature and reaction time

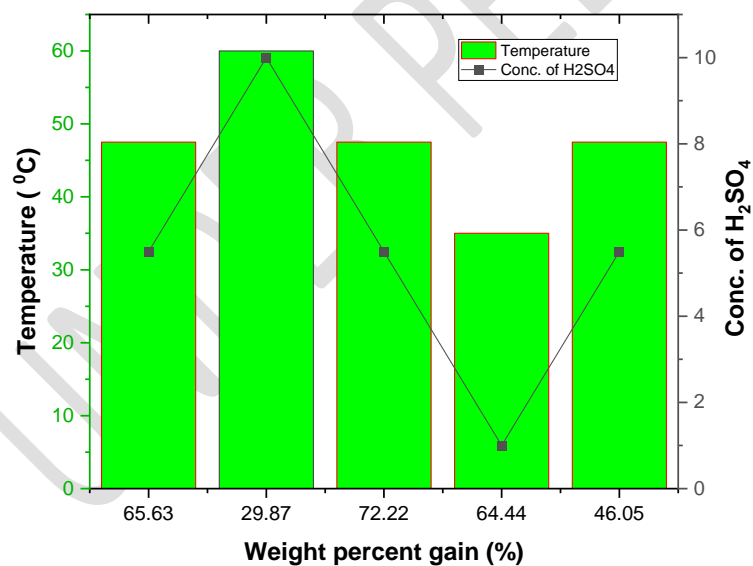


Fig 9: A plot of WPG of acetylated cellulose as a function of temperature and catalyst concentration

CONCLUSION

In this investigation, CNCs were successfully extracted from bean seed hulls via sulphuric acid hydrolysis. Prior to this, the non-cellulosic components such as lignin, pectin, wax and hemicellulose were extensively removed by alkali treatment and bleaching. The chemical composition study reveals higher percentage of raw cellulose content with a lower percentage of lignin, hemicellulose and ash content. The reduced moisture content of CTA than that of CNCs means that CTA will make a better biofuel than CNCs. The percentage yield suggests that large quantity of CNCs will be employed to obtain a greater yield of CTA. The solubility test showed that both the isolated CNCs and CTA were sparingly soluble in the polar solvent, water but insoluble in the organic solvent, ethanol. Some functional groups related to lignin and hemicellulose were identified using FTIR spectrometer implying that the pretreatment process did not remove all the lignin and hemicellulose from the isolated CNCs. The SEM analysis showed that the extracted CNCs has a magnified specific surface area and pore size than CTA making CNCs a better adsorbent than CTA. Therefore, CNCs obtained from bean seed hulls have great potential to be utilized as adsorbent for heavy metals, crude oil, dyes, pesticides etc. as well as to be converted into CTA fabrics thereby remediating environmental pollution emanating from bean seed hulls.

REFERENCES

- [01] O.P Nsude, K.J Orie. Thermodynamic and adsorption analysis of corrosion inhibition of mild steel in 0.5M HCl medium via ethanol extracts of *Phyllanthus mellerianus*. *American Journal of Applied Chemistry*, 10(3), (2022),67-75.
- [02] M. Auffhaminer , V. Ramanathan, J. Vincent. *Proceedings of the National Academy of Science*. 5(52),(2006), 19668-19672.
- [03] Agarwal B. (2009). Gender and forest conservation: the impact of women's participation in community forest governance. *Ecological economies* 68(11), (2009),2785-2799.
- [04] C.C Nwajiobi, J. Otaigbe, O. Oriji. Isolation and Characterization of microcrystalline cellulose from papaya stem. *Der Pharma Chemica* 11(3), (2019), 19-26
- [05] O.P Nsude, K.J Orie, P.I Udeozo, O. Ogbobe and C.C Chime. Isolation, physicochemical and BET analysis of cellulose from *Pentaclethra macrophylla* Benth (Oil Bean) Pod Biomass

Wastes International Research Journal of Pure and Applied Chemistry. 23(5), (2022), 9-22.
Doi:10.9734/IRJPAC/2022/v23i530474.

[06] A.S Aridi, Y.A Yusuf , L.C Nyuk, N.A Ishak and Y.N.N Mohammad Yusuf. Isolation of cellulose from *Leucaena leucocephala* mature pods and how different bleaching agents affect its characterization. *Materials performance and characterization*, 11(1), (2022), 236-243.

[07] T.C Onuegbu. Improving fuel wood efficiency in rural Nigeria: Briquette technology chemistry in Nigeria. *A National Magazine in the chemical society of Nigeria*. 4(3), (2010), 35-39

[08] B.C Saha. Hemicellulose bioconversion. *Journal of industrial microbiology and biotechnology*, 30, (2003), 279-291

[09] R.G Candido, G.G Godoy and A.R Goncalves. Study on sugarcane bagasse pretreatment with sulphuric acid as a step of obtaining cellulose. *WASET*, 61, (2012), 101-105

[10] A. Bello, M.T Isa, B.O Aderemi, and B. Mukhtar (2016). Acetylation of cotton stalk for cellulose acetate production. *American Scientific Research Journal for Engineering, Technology and Sciences (ASRJETS)*, 15(1): 137-150

[11] R. Malladi, M. Nagalakshmaiah, M. Robert and S. Elkoun. Importance of agricultural and industrial waste in the field of nanocellulose and recent industrial developments of wood based nanocellulose: A review. *ACS Sustainable Chemistry & Engineering*,(2018), Pp 1-70.
Doi:10.1021/acssuschemeng.7b03437

[12] D. Klemm, F. Kramer, S. Moritz, T. Lindstrom, M. Ankerfors, D. Gray, A. Dorris. Nanocelluloses: A New Family of Nature-Based Materials. *Angew. Chem. Int. Ed.* 50(24), (2011), 5438-5466. Doi:10.1002/anie.201001273

[13] I.L Finar. *Organic chemistry: Stereochemistry and the chemistry of natural products*. Vol 2, 5th Edition. Pearson Education Limited, 2014, pp 350-353

[14] M.M De Souza Lima, R.R Borsali. Cellulose microcrystals: structure, properties and applications. *Macromol. Rapid Commun.* 25(7),2004, 771-789. Doi: 10.1002/marc.200300268

- [15] R.M Sheltami, T. Abdullah, I. Ahmad, A. Dufresne and H. Kargarzadeh. Extraction of Cellulose nanocrystals from mengkuang leaves (*Pananus tectorius*). *Carbohydrate Polymers* 88(2), (2012), 772-779. <https://doi.org/10.1016/j.carbpol.2012.01.062>
- [16] Y. Habibi, L. Lucia and O. Rojas. Cellulose nanocrystals: Chemistry self-assembling and applications *chemical reviews*, 110(6), (2010), 3479-3500. Doi:10.1021/cr900339w
- [17] X. He, F. Luzi, W. Yang, Z. Xiao, L. Torre, Y. Xie and D. Puglia. Citric Acid as green modifier for tuned hydrophilicity of surface modified cellulose and lignin nanoparticles. *ACS Sustainable chemistry and engineering*. 6(8), (2018), 9966-9978. <https://doi.org/10.1021/acssuschemeng.8b01202>.
- [18] D. Plackett & A. Sodergard. *Natural fibres, biopolymers and biocomposites*. CRC Press, Boca Raton, 2005, pp 569
- [19] W. Yang, E. Fortunate, F. Luzi, J.M Kenny, L. Torre and D. Puglia. Lignocellulosic /Based Bionanocomposites for Different Industrial Applications. *Current Organic Chemistry*, 22(12), (2018), 1205-1221. <https://doi.org/10.2174/1385272822666180515120948>
- [20] R.T Morrison, R.N Boyd and S.K Bhattacharjee. *Organic chemistry*. 8th Edition, Dorling Kindersley (India) Pvt. Ltd, 2018, Pp 1267, 1274-1276.
- [21] J. Lamaming, R. Hashim, C.P Leh, O. Sulaiman, T. Sugimoto, M. Nasir. Isolation and characterization of cellulose nanocrystals from parenchyma and vascular bundle of oil palm trunk (*Elaeis guineensis*). *Carbohydrate polymers*, 88(2), (2012), 772-779
- [22] F. Luzi, D. Puglia, F. Sarasini, J. Tirillo, G. Maffei, A. Zuorro, R. Lavecchia, J.M Kenny, L. Torre. Volarization and extraction of cellulose nanocystals from North African grass: *Ampelodesmos Mauritanicus* (Diss). *Carbohydrate Polymers* 209, (2019), 328-337. <https://doi.org/10.1016/j.carbpol.2019.01.048>
- [23] I.A Sacui, R.C Nieuwendaal, D.J Burnett, S.J Stranick, M. Jorfi, C. Weder, F.E Johan, R.T Olsson, & J.W Gilman. Comparison of the properties of cellulose nanocrystals and cellulose nanofibrils isolated from bacteria, tunicate and wood processed using acid, enzymatic, mechanical and oxidative methods. *ACS Applied materials and interfaces*, 6(9), (2014), 6127-6138. <https://doi.org/10.1021/am500359f>

- [24] R.M Matos, J.Y Cavaillé, A. Dufresne, J.F Gerard, &C. Graillat. Processing and Characterization of new thermoset nanocomposites based on cellulose whiskers. *Composite interfaces*, 7(2), (2000), 117-131. <https://doi.org/10.1163/156855400300184271>
- [25] M. Neus Anglés, &A. Dufresne. Plasticized starch/ tunicin whiskers, nanocomposite materials.2. Mechanical behaviours. *Macromolecules*, 34(9), (2001), 2921-2931. <https://doi.org/10.1021/MA001555H>
- [26] Y. Xiao, Y. Liu, X. Wang, M. Li, H. Lei, H. Xu. Cellulose nanocrystals prepared from wheat bran: characterization and cytotoxicity assessment. *International Journal of biological macromolecules*, 140, (2019), 225-233
- [27] Z. Kassab, Y. Abdellaoui, M.H Salim, M. El Achaby. Cellulosic Materials from *Pealpisum sativum* and broad beans (*vicia faba*) pods agro-industrial residues. *Material Letters* 280, (2022), 128539. [https://doi.org/10.1016\(j.matlet.2020.128539\)](https://doi.org/10.1016/j.matlet.2020.128539).
- [28] B.S Furniss, A.J Hannaford, P.W.G Smith, A.R Tatchell. *Vogel's textbook of practical organic chemistry*. 5th Edition. Pearson Education limited, England, 1989, pp 1196-1204, 1225, 1289-1398.
- [29] ASTM International. ASTM D792-17 Standard test methods for density, specific gravity (Relative Density of plastics by displacement), cellulose, lignin, hemicellulose, moisture content and melting point. West Conshohocken, PA: ASTM International, 2017.
- [30] American Oil Chemists' Society (AOAC). *Official methods and recommended practices of the AOCS* (7th ed.). AOCS Press, 2017.
- [31] ASTM International. ASTM E70-18 Standard Test for pH of aqueous solutions with the glass electrode. West Conshohocken, PA: ASTM International, 2015.
- [32] C.I Azogu. *Laboratory Organic Chemistry: Techniques, qualitative analysis, organic preparations and spectroscopy*. 2nd Edition. Maybinson Book Publishers, New Jersey, USA, 2010, pp 153-200.
- [33] I.A Ajayi, R.A Oderinde, D.O Kajogbola, J.I Uponi. Oil content and fatty acid composition of some underutilized legumes from Nigeria. *Journal of Food Chemistry* 99, (2006), 115-120. Doi:10.1016/j.foodchem.2005.06.045.

- [34] M. Ibourki, F. Azouguigh, S. Jadouali, E. Saka, L. Bijla, K. Majourhat, S. Gharby, and A. Lahnifli. Physical fruit traits, nutritional composition and seed oil fatty acid profiling in the main date palm (*Phoenix dactylifera* L.) varieties grown in morocco. *Hindawi Journal of Food Quality*. Vol 2021, Article ID5138043, 12pages. <https://doi.org/10.1155/2021/5138043>.
- [35] A. Alkinjokun, L.F Petrik, J. Ogunfowokan, J. Ajao, &T.V Ojumu. Isolation and characterization of nanocrystalline cellulose from cocoa pod husk (CPH) biomass wastes. *Heliyon*, 7(4), (2021), e06680
- [36] M.H Alhaji, E.N Oparah, M.K Yakubu, C.C Maju, H. Suleiman, I. Akawu, T.A.D Musa and S. Aliyu. Production, properties and applications of cellulose/waste leather buff composite (WLB) for environmental sustainability and recyclability. *Journal of Chemical Society of Nigeria*, 46(3), (2021), 610-617. <https://doi.org/10.46602/jcsn.v46i3.634>
- [37] W.L Danbature, Z. Shehu, J. Joshua. and M.M Adam. Moringa oleifera root-mediated synthesis of nanosilver particles and the antibacterial applications. *Journal of Chemical Society of Nigeria*, 46(3), (2021), 504-516. <https://doi.org/10.46602/jcsn.v446i3.626>
- [38] M.O Ekeoma, P.A.C Okoye P.A.C, V.I.E Ajiwe&B.H Hameed. Modified coconut shell as active heterogeneous catalyst for the transesterification of waste cooking oil. *J. Chem. Soc. Nigeria*, 45(2), (2020), 360-368
- [39] A.A Pam, A.A Adeyi, G.K Obiyenwa, I. Yinusa, &O.W Salawu. Adsorption of methylene blue from aqueous solution using iminodiacetic acid supported montmorillonite adsorbent. *J. Chem. Soc. Nigeria*, 45(2), (2020), 288-297.
- [40] R. Saravanan and I. Ravikumar. The use of new chemically modified cellulose for heavy metal ion adsorption and antimicrobial activities. *Journal of Water Resources and Protection*, 7, (2015), 530-545
- [41] D.H Williams and I. Fleming. *Spectroscopic methods in organic chemistry*. 3rd Edition. McGraw-Hill Book Company (UK) Limited England, 1980, pp 47-73
- [42] M.U Akpuaka. *Essentials of Natural Products Chemistry*. 1st Edition. Mason Publishers Enugu, Nigeria, 2009, pp 25-30.

[43] www.vedantu.com/chemistry/us... Retrieved on the 1st of August 2023 at 03:20am West Central African Time.

[44] G.I Badea and G.L Radu. Introductory chapter: Carboxylic acids-keyrole in life Sciences, 2018,<https://dx.doi.org/10.5772/intechopen.77021>

[45] A.S Kalgutkar, J.S Daniels. Carboxylic acids and their bioisosteres. In: Metabolism, pharmacokinetics and toxicity of functional groups: impact of the building blocks of medicinal chemistry on ADMET. London: Royal Society of Chemistry, (2010), pp 99-167

[46] A.R Pfaff, J. Beltz, E. King &N. Ercal. Medicinal thiols: current status and new perspectives Mini Rev. Med. Chem. 20(6), (2020), 513-529. Doi:10.2174/1389557519666191119144100

[47] A. Smith. Nova Biomedical: The importance of ketones from a clinical and medical perspective. News-Medical, (2023).<https://www.newsmedical.net/news/20230308/The-importance-of-ketones-from-a-clinical-and-medical-perspective.aspx>.

[48] A. Carter&T. Jewel. What are the medical and health uses of phenol? An overview. Healthcare, (2019)

[49] H.H Al Mamari. Phenolic compounds: classification, chemistry and updated techniques of analysis and synthesis. Chapter metrics overview. Open access peer-reviewed chapter. Healthline media, (2021), Doi:10.5772/intechopen-98958.

[50] C.W Haminiuk, G.M Maciel, M.S.V Plata-Oviedo, R.M Peralta. Phenolic compounds in fruits- an overview. Food Sci. Technol. Int., 47, (2012) 2022-2044. <https://doi.org/10.1111/j.13652621.2012.03067.x>

[51] S. Das, J. Das, A. Samadder, A.R Khuda- Bukhsh. Dihydroxy –isosteviol methyl ester from *pulsatilla nigricans* induces apoptosis in Hela cells: its cytotoxicity and interaction with calf thymus DNA. Phototherapy Research 27(5), (2012), 664-673. <https://doi.org/10.1002/ptr.4768>

[52] Y. Wang &H. Qian. Pthalates and their impacts on human health. Healthcare 9(5), (2021), 603. Doi:1.3390/healthcare9050603

[53] W. Ericson-Neilsen &A.D Kaye. Steroids: Pharmacology, complications and practice delivery issues. The Ochsner Journal, 14(2), (2014), 203-207.

- [54] S. Sharma & N. Anand. Approaches to design and synthesis of antiparasitic drugs. *Pharmacochemistry library*. Vol 25, (1997), pp 296-324. [https://doi.org/10.1016/S0165-7208\(97\)80034-7](https://doi.org/10.1016/S0165-7208(97)80034-7)
- [55] B.Y.S Negi. Studies on cellulose nanocrystals isolated from groundnut shells. *Carbohydrate Polymers* 157, (2017), 1041-1049
- [56] T. Carreón and R.L Herrick. *Aliphatic hydrocarbons*. Wiley Online Library, (2012). <https://doi.org/10.1002/0471435139.tox049.pub2>
- [57] www.google.com. Retrieved on the 1st of August 2023 at 2:30am West Central African Time
- [58] G. Dumonteil & S. Berteina-Rabolo. Synthesis of conjugated dienes in natural compounds. *Journals Catalysis*, 12(1), (2022), 86. [Doi.org/10.3390/catal12010086](https://doi.org/10.3390/catal12010086)
- [59] A. Rani, S. Jain, R. Kumar & A. Kumar. 1,5-Bis (2-hydroxyphenyl) pent-1,4-diene-3-one: A lead compound for the development of broad-spectrum anti-bacterial agents. *S. Afr. J. Chem.* 63, (2010), 31-35. <https://journals.sabinet.co.za/sajchem/>
- [60] N.W.P Flauzino, H.A Silverio, N.O Dantas, D. Pasquini. Extraction and characterization of cellulose nanocrystals from agro-industrial residue-soy hulls, *Ind. Crop Prod.* 42, (2013), 480-488.
- [61] J. George; S. SN. Cellulose nanocrystals: synthesis, functional properties and applications. *Nanotechnology Sci. Appl.* (2015). [Doi: 10.2147/NSA.S64386](https://doi.org/10.2147/NSA.S64386)

UNDER PEER REVIEW